

Scientific paper

Modeling of Calcium Leaching from Cement Hydrates Coupled with Micro-Pore Formation

Kenichiro Nakarai¹, Tetsuya Ishida² and Koichi Maekawa³

Received 1 February 2006, accepted 1 September 2006

Abstract

A computational system for predicting the long-term degradation of cement hydrates due to calcium leaching is presented. The leaching of calcium ions from hardened cement hydrates is simulated as the multi-phase equilibrium of calcium in solid and liquid phases and their transport is formulated on the basis of thermodynamics. The time-dependent properties of cement hydrates associated with hydration, pore-structure development, and moisture transport are evaluated by integrating calcium leaching and statistical models of chemo-physics. The proposed model delivers reasonable predictions of calcium leaching in high-performance concrete with a low water-to-cement ratio as self-curing takes place.

1. Introduction

The applicability of concrete as a solidifying barrier for the geological disposal of radioactive waste is being studied. Radioactive waste contains materials with long half-lives, so the period of stability required in design is several tens of thousands of years. This far exceeds the expected lifetime of the regular infrastructure. Calcium leaching over such an extremely long service life is one issue of crucial importance to be considered in the design and planning of such projects. The prediction of such phenomena over very long periods is difficult through experiments or accelerated tests alone. Experimental methods need to be combined with numerical analysis for more rational evaluations of performance, since methods of assessing barriers on a real-time scale are not realistic. In feasibility studies as well as actual design, numerical simulations that take a rational approach to account for mix proportion, types of constituent materials, structural dimensions, and detailing are greatly useful. In other words, a theoretical schema plays an essential role in linking accelerated tests with reality.

Degradation due to calcium leaching has been reported since the 1920s. Despite this, there have been few cases in which ordinary structures suffered from calcium leaching damage because the rate of degradation is relatively slow compared with carbonation, chemical attack, and corrosive reactions. In a few cases, degradation caused by leaching has been observed in hydropower installations and facilities related to water supply after long-term service of approximately 100 years. From a

practical viewpoint, safety verifications related to calcium leaching from cement hydrates are unnecessary for cementitious composites in normal use. Consequently, the recent need to investigate long-term degradation caused by calcium leaching can be seen as a new challenge on the road to developing artificial safety barriers for nuclear waste depositories.

In this study, a new model of calcium leaching is proposed. The key issue is the analysis of a transient process in which the microstructure of cement hydrates varies in time and space. Calcium leaching generally results in a coarser micro-pore structure that allows easier mass transport. At the same time, the newly created voids may form new spaces in which additional cement hydration can take place. Calcium leaching and the evolving microstructure are strongly coupled with each other, and both need to be simulated in order to realize performance assessments of cement composites over extremely long periods of time. By integrating a calcium ion transport model with a statistical micro-structural model of chemo-physics, the aim is to achieve wide applicability to cover an arbitrary choice of mix proportion, constituent material characteristics, and ambient conditions. Systematic experimental verification and validation of the proposed model are also reported.

2. Modeling of calcium leaching

2.1 Thermodynamics analysis system

Calcium leaching from cement hydrates correlates strongly with the processes of cement hydration, microstructure formation, and moisture distribution (**Fig. 1** and **Fig. 2**). As these chemo-physical processes are highly time-dependent, the consequent microscopic and macroscopic properties of cement composites can be treated as variables. A computational method has been developed for the simulation of such transient chemo-physical processes (Maekawa *et. al* 1999). This scheme is used as the basis for this study. It consists of a multi-component hydration model, a moisture transport/equilibrium model,

¹Assistant Professor, Department of Civil Engineering, Gunma University, Japan.

E-mail: nakarai@ce.gunma-u.ac.jp

²Associate Professor, Department of Civil Engineering, University of Tokyo, Japan.

³Professor, Department of Civil Engineering, University of Tokyo, Japan.

and a micro-pore structure development model. Through several verifications, it has been proved that early-age development processes such as heat generation and moisture profile, can be simulated for arbitrary mix proportions and ambient conditions. In addition, the analytical system has been extended to allow prediction of the mid-term durability of reinforced concrete in regard to the penetration of chloride ions and carbon di-

oxide, as well as the corrosion of embedded steel (Ishida and Maekawa 2000, Maekawa *et al.* 2003).

In this study, a model of calcium leaching is overlaid over this analytical scheme (Fig. 1). This enables the strong interaction between calcium leaching and the micro-macro solid features of concrete to be consistently taken into account (Fig. 2).

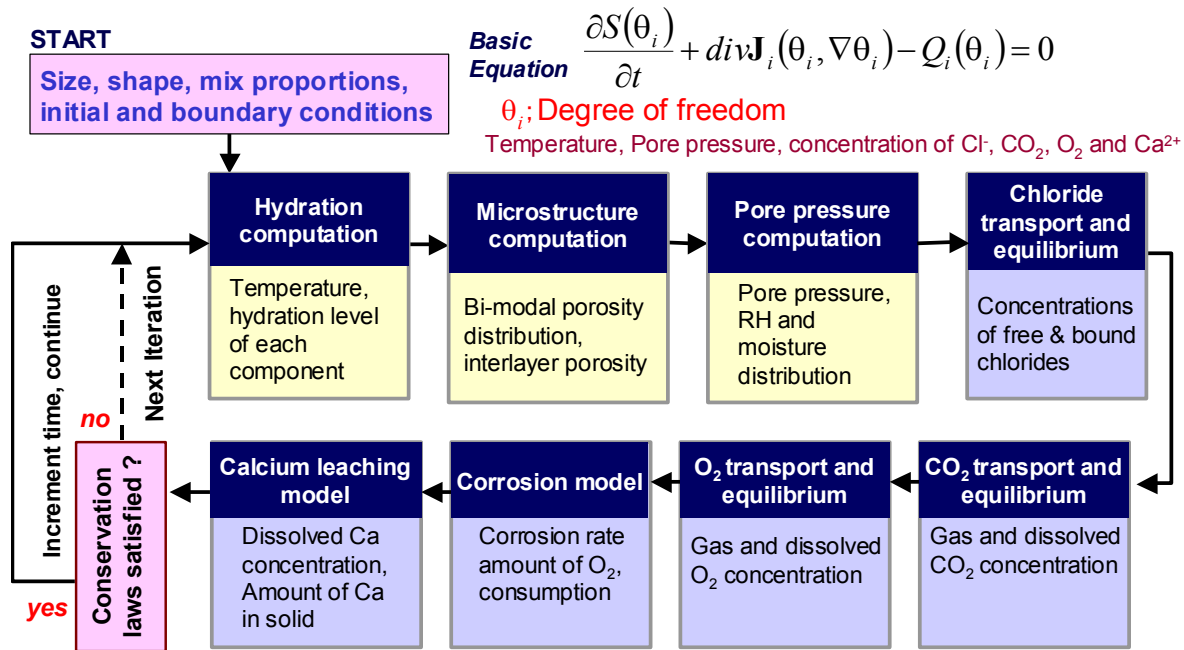


Fig. 1 Overall scheme of DuCOM chemo-physical coupled system.

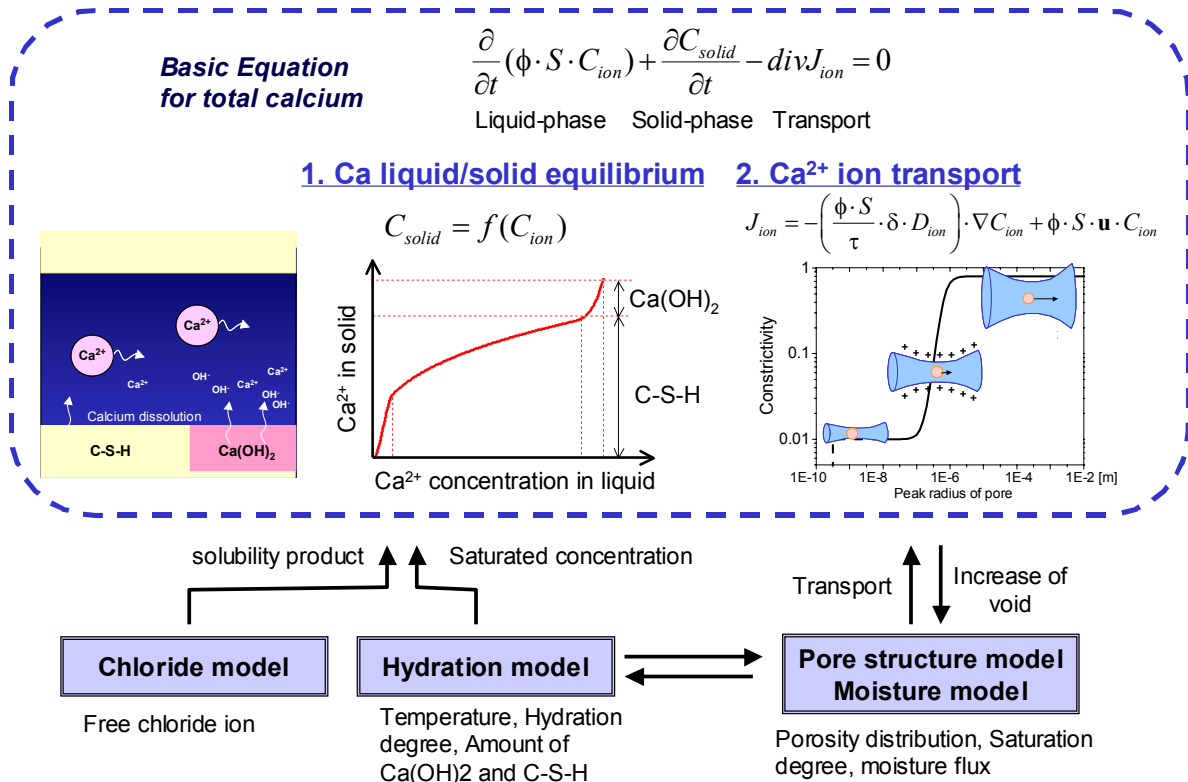


Fig. 2 Calcium leaching model coupled with time-dependent material properties.

2.2 Law of conservation of mass for calcium

Momentum, energy, and material flows must satisfy the conservation laws. As the governing equation for calcium, we have mass conservation Equation (1) as given below. This relates the total mass of calcium in the pore solution and the solid phase calcium in the system. It was originally formulated by Gérard *et al.* (2002) as,

$$\frac{\partial}{\partial t}(\phi \cdot S \cdot C_{ion}) + \frac{\partial C_{solid}}{\partial t} - \text{div}J_{ion} = 0 \quad (1)$$

where, ϕ is porosity [m^3/m^3], S is degree of saturation, C_{ion} is the molar concentration of calcium ions in the liquid phase [mmol/m^3], C_{solid} is the amount of calcium in the solid phase [mmol/m^3], and J_{ion} is the flux of calcium ions [$\text{mmol}/\text{m}^2\text{-s}$].

The first and second terms of Equation (1) represent the increments in the amount of calcium in the liquid and solid phases per unit time and volume, respectively. The relation between calcium ion concentrations in the liquid and solid phases is given by the solid-liquid equilibrium model, as described later. Phase transformation (i.e. dissolution from solid to liquid phases or precipitation from liquid to solid phases) is implicitly expressed by assuming a quasi-equilibrated process. The third term of the equation represents the diverging mass flux. The calcium ion flux at a specific boundary surface is expressed by,

$$q_S^{Ca} = -h_{Ca} (C_{ion} - C_{ion_S}) \quad (2)$$

where, q_S^{Ca} represents the flux of calcium ions into the porous medium at the surface [$\text{mmol}/\text{m}^2\text{-s}$], h_{Ca} is the surface calcium ion emissivity coefficient [m/s], and C_{ion_S} is the environmental concentration of calcium ions [mmol/l]. The value of the coefficient is assumed to be 1.0×10^{-3} [m/s], the same as the surface chloride ion emissivity coefficient in the chloride model (Ishida and Maekawa 2000).

2.3 Solid-liquid equilibrium for calcium

As for the thermodynamic equilibrium of calcium in the solid and liquid phases, an isotherm correlation proposed by Buil's *et al.* (1992) is installed with minor modifications for computational efficiency as shown in Fig. 3. As the original Buil's model has a simple mathematical formulation with reasonable accuracy, it has been widely used by other researchers (ex. Yokozeki *et al.* (2003)). In this study, the original Buil's model was slightly modified so as to uniquely determine the quantity of solid calcium from a given ion concentration in the pore solution. In this modification, the mathematical formulation adopted by Gérard *et al.* (2002) was referred to and the consistency of the model with the experimental data earned by Berner (1988) was maintained as,

$$C_{Solid} = f(C_{ion}) = A \cdot \left\{ C_{CSH} \cdot (C_{ion}/C_{sat})^{1/3} \right\} + B$$

$$A = \begin{cases} -\frac{2}{x_1^3} C_{ion}^3 + \frac{3}{x_1^2} C_{ion}^2 & (0.0 \leq C_{ion} \leq x_1) \\ 1 & (x_1 < C_{ion}) \end{cases} \quad (3)$$

$$B = \begin{cases} 0 & (0.0 \leq C_{ion} \leq x_2) \\ \frac{C_{CH}}{(C_{sat} - x_2)^3} \cdot (C_{ion} - x_2)^3 & (x_2 < C_{ion}) \end{cases}$$

where, C_{CSH} is the amount of calcium in the solid phase of the C-S-H gel [mmol/m^3], C_{CH} is the amount of calcium in the solid phase of the calcium hydroxide [mmol/m^3], C_{sat} is the saturated liquid phase calcium ion concentration [mmol/l], x_1 is the liquid phase calcium ion concentration when the rapid transition of C-S-H gel into silica gel begins [mmol/l], and x_2 is the liquid phase calcium ion concentration when the calcium hydroxide has completely dissolved and the dissolution of C-S-H gel begins [mmol/l].

In this research, $x_1 = 2.0$ mmol/l and $x_2 = (C_{sat} - 3.0)$ mmol/l are adopted. Since calcium hydroxide has the highest solubility among the hydrates in the leaching process, it dissolves first. During dissolution, the calcium ion concentration of the solution gradually decreases to x_2 from C_{sat} . After the calcium hydroxide is lost, dissolution of C-S-H gel starts. As the dissolution of the C-S-H gel proceeds and the liquid phase calcium ion concentration falls below x_1 , the C-S-H gel decomposes rapidly into silica gel. Here, the presence of alkali salts such as sodium and potassium is ignored. But, the presence of sodium chloride is implicitly taken into account through the change in solubility product, as described later, since it is known that sodium chloride accelerates calcium leaching (Imoto *et al.* 2004).

The parameters in the phase equilibrium (i.e. the amount of calcium and the saturated concentration of calcium ions) are defined not through experiments but by computation. All are calculated as time-dependent variables in order to take into account the influence of mix proportion, ambient conditions, hydration, and degradation due to calcium leaching.

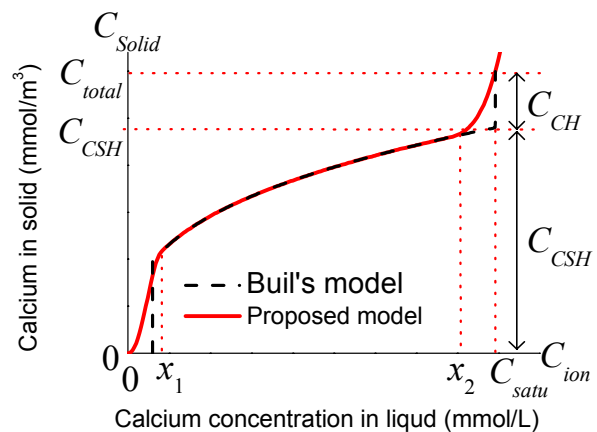
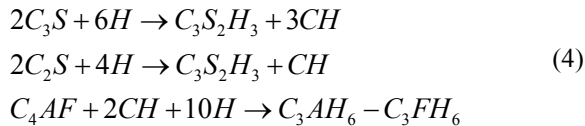


Fig. 3 Solid-liquid equilibrium model for calcium.

The total amount of calcium in the solid phase of the cementitious composite is determined from the chemical composition of the mixture. The amount of calcium in the fly ash and blast furnace slag is obtained from the CaO content, which is assumed to be present at a ratio of 41.8% (JSCE 1988a) and 4.4% (JSCE 1988b), respectively. The amount of calcium hydroxide in the cement paste is determined stoichiometrically using the following equations in the multi-component hydration model (Maekawa *et al.* 1999):



When using fly ash and blast furnace slag as admixtures, calcium hydroxide is consumed in the reaction. Consumption is assumed to be 100% and 22% in the case of fly ash and blast furnace slag, respectively (Maekawa *et al.* 1999).

The concentration of saturated calcium ions in the liquid phase equates to the concentration of saturated calcium hydroxide in the pore solution in this study. This is a simplified treatment neglecting the presence of coexisting ions such as sodium and potassium. By assuming that no other ions coexist with the calcium ions derived from the calcium hydroxide, the electroneutrality rule gives the concentration of saturated calcium ions from the solubility product as,

$$C_{satu} = \frac{1}{2} \sqrt[3]{2K_{sp}} \quad (5)$$

where, C_{satu} is the concentration of saturated calcium ions [mmol/l] and K_{sp} is the solubility product of calcium hydroxide [mmol³/l³]. In order to account the effects of temperature and sodium chloride concentration, the solubility product is corrected by adding the contribution of sodium chloride to the change in solubility product, ΔK_{sp}^{Cl} , to the solubility product including the effect of temperature, K_{sp}^T , as given by the following equation:

$$K_{sp} = K_{sp}^T + \Delta K_{sp}^{Cl} \quad (6)$$

where, K_{sp}^T is the solubility product of calcium hydroxide considering the effect of temperature [mmol³/l³] and ΔK_{sp}^{Cl} is a term for the effect of sodium chloride on the solubility product of calcium hydroxide [mmol³/l³]. For the temperature effect, the following approximation (Fig. 4) is derived from the literature (CSJ 2004):

$$K_{sp}^T = 0.0125 \times 10^9 \cdot e^{-0.019T} \quad (7)$$

where, T is absolute temperature [K]. As a matter of fact, much less data is available for deep discussion on the effect of sodium chloride. Then, in this study, the concentration of saturated calcium was measured for different sodium chloride solutions, and the term ΔK_{sp}^{Cl} was experimentally identified. Here, the authors tentatively

propose a simple model having the explicit formulae on the direct basis of experiment as shown in Fig. 5. It should be noted that there is still a possibility of different dissolution of calcium oxide in this experiment from that of calcium oxide in the real cement hydrate. In order to further discuss the ion interaction as the first stage, the simple modeling is of great importance to conduct the system simulation of calcium leaching from cement composites and compare the derived phenomena with the reality in multiple views. Then, we have,

$$\begin{aligned} \Delta K_{sp}^{Cl} &= A' \cdot (5 \times 10^4 \cdot \sqrt[3]{Cl}) \\ A' &= \begin{cases} -2Cl^3 + 3Cl^2 & (0.0 \leq Cl \leq 1.0) \\ 1 & (1.0 < Cl) \end{cases} \end{aligned} \quad (8)$$

where, Cl is the concentration of sodium chloride in the pore solution [mass%]. The concentration of free chloride ions determined from the chloride ion transport model (Ishida and Maekawa 2000, Maekawa *et al.* 2003) is taken to be the concentration of sodium chloride in the analysis system. Concerning the computational phase-equilibrium formulae, the sensitivity with respect to the perturbation of chloride ion is intentionally set small for computational stability of highly nonlinear range of the solubility product at the low chloride ion

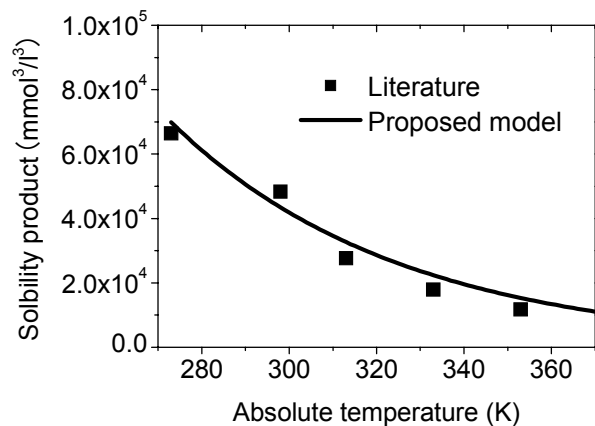


Fig. 4 Influence of temperature on solubility product.

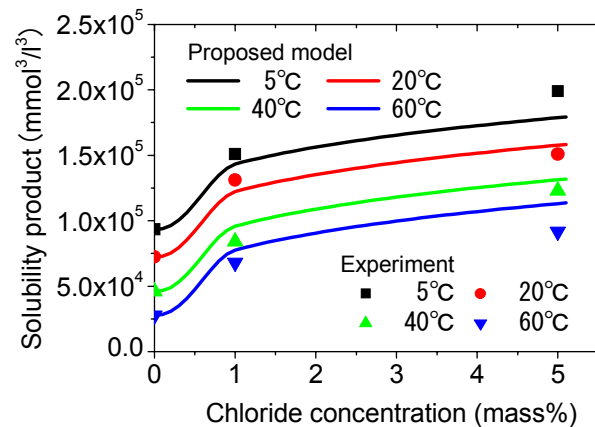


Fig. 5 Influence of chloride ions on solubility product.

concentration as well as the chemo-physical accuracy.

2.4 Transport of calcium ions

By considering both diffusion and advection (Ishida and Maekawa 2000), the flux of calcium ions transported in a porous media is written as (see Fig. 2),

$$J_{ion} = -\left(\frac{\phi \cdot S}{\tau} \cdot \delta \cdot D_{ion}\right) \cdot \nabla C_{ion} + \phi \cdot S \cdot \mathbf{u} \cdot C_{ion} \quad (9)$$

where, τ is tortuosity, δ is constrictivity, D_{ion} is the diffusion coefficient of a calcium ion [m^2/s], $\nabla^T = [\partial/\partial x \ \partial/\partial y \ \partial/\partial z]$ is the nabla operator, and $\mathbf{u}^T = [u^x \ u^y \ u^z]$ is the velocity vector of a calcium ion transported by solution flow [m/s]. By treating the capillary and gel pores in the cement paste as ion transport pathways, the porosity, ϕ , is expressed by the following equation (Ishida and Maekawa 2000):

$$\phi = \phi_{cp} + \phi_{gl} \quad (10)$$

where, ϕ_{cp} and ϕ_{gl} are the porosities of capillary and gel pores, respectively. Here, it is assumed that no ion is transported into the interlayer pores of the cement paste since the molecular-related size of the interlayer space is too small to allow substantial room of any ion.

The first term of Equation (9) represents the component of molecular diffusion, while the second is a component representing advection driven by the flow of condensed liquid water in the pore. The velocity of calcium ions related to advection is assumed to reflect the bulk motion of the condensed water; it is determined from the transport model for the liquid phase. The diffusion coefficient of calcium ions is expressed according to Einstein's theorem by,

$$D_{ion} = R \cdot T \cdot \frac{\lambda_{ion}}{Z_{ion}^2 \cdot F^2} \quad (11)$$

where, R is the ideal gas constant [$\text{J/mol}\cdot\text{K}$], λ_{ion} is the molar conductivity of an ion [Sm^2/mol], Z_{ion} is the ion valence ($=2$), and F is the Faraday constant [C/mol]. Regarding the molar conductivity of an ion, λ_{ion} , temperature dependency is taken into account by the Arrhenius law (Yokozeki *et al.* 2003) as,

$$\lambda_{ion} = \lambda_{ion_{25}} \cdot \exp\left\{-1700\left(\frac{1}{T} - \frac{1}{298}\right)\right\} \quad (12)$$

where, $\lambda_{ion_{25}}$ is the molar conductivity of an ion at 25°C (CSJ 2004).

Ion transport in a porous media like concrete is affected by the micro pore structure. In this study, the effect of pore structure is expressed in terms of porosity, degree of saturation, tortuosity, and constrictivity (Atkinson and Nickerson 1984). Tortuosity is defined as a function of porosity, while constrictivity is a function of pore radius.

Tortuosity is formulated first. It expresses the in-

creased length of actual ion transport pathways in accordance with the geometrical connectivity of pore spaces. Tortuosity is thought to be higher for cement paste with finer pores at lower W/C ratios and lower at larger W/C ratios or where coarse pores have been caused by leaching. The tortuosity of pores in the cement paste, τ_{paste} , is assumed to be expressed in terms of effective porosity, ϕ_{paste} , using Equation (8) as an analogy with past research on chloride ion diffusion coefficients (Maekawa *et al.* 2003; see Fig. 6). This is because the tortuosity is an intrinsic characteristic expressing the geometrical property of pore structure and it can be assumed to be independent on the characteristics of ions.

$$\tau_{paste} = -1.5 \tanh\{8.0(\phi_{paste} - 0.25)\} + 2.5 \quad (13)$$

$$\phi_{paste} = \frac{\phi_{cp} + \phi_{gl}}{V_{paste}}$$

where, ϕ_{paste} is the effective porosity representing the sum of gel and capillary pores effective as ion transport pathways per unit volume of cement paste [m^3/m^3] and V_{paste} is the unit volume ratio of cement paste [m^3/m^3]. Here, the equation was proposed as a function of porosity by modifying the original model with regard to the peak radius of capillary pores. In the modification, the relation between the porosity and the peak radius was examined by the sensitivity analysis beforehand.

Next, constrictivity is formulated as an expression of the effect of pore size. Porosity and pore size distribution were taken into account in one past study of constrictivity (Van Brakel and Heerijes 1974). Pore dimensions are thought to be the main determinant of constrictivity (Atkinson 1984). A significant range of constrictivities has been reported, with a value of about 0.8 for ordinary porous materials (Van Brakel 1974, Petersen 1958) but of the order of about 0.01 for fine pores in cement paste (Atkinson 1984). In order to determine the value of the constrictivity for the sound and deteriorated cement paste, the interaction between pore structure and ion transport needs to be discussed.

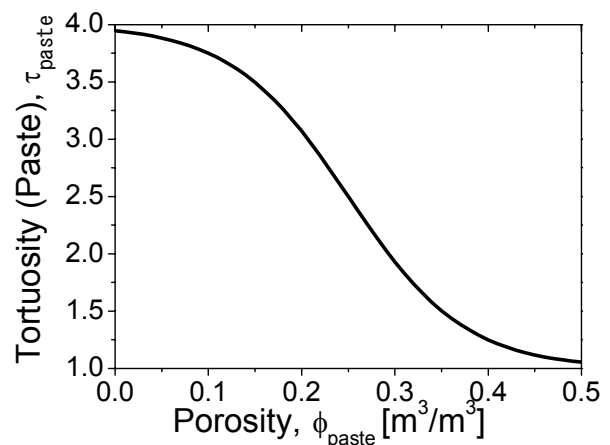


Fig. 6 Modeling of tortuosity for cement paste.

Pores in cement paste are widely distributed over the nanometer-to-micron scale and pores with varying dimensions are randomly connected. The average rate of ion transport is thought to be lower in fine pores because of interactions between the ions and pore walls in addition to the size factor. Electrical interactions between ions and pore walls have been cited as a reason for this (Sato *et al.* 1995). The pore walls in cement paste are positively charged, as are the calcium ions. Therefore, the effective dynamic pathway may be reduced in size due to electrostatic repulsion. This effect depends on the ion type, the ion concentration, and other factors, but is largely dependent on pore size and ion radius. The smaller the pore size is, the more dominant the electrostatic effect (Sato *et al.* 1995). Accordingly, one fine pore in a connected series of pores within the cement hydrate can hinder ion transport strongly, so pore constrictivity becomes prominent in cement paste (Fig. 7). The reduced transport resulting from pore connectivity and this interaction between ions and pore walls is expressed as constrictivity in this study.

On the other hand, in the large pores of ordinary porous media such as soils and severely deteriorated cement paste, this sort of interaction becomes less but the constrictivity becomes larger. Based on the above discussion, the constrictivity of pores in a cement paste is defined with respect to the peak pore radius by Equation (14) (Fig. 8). The equation gives a value of 0.01 for the fine pores in the sound cement paste, whereas it gives a value of 0.8 for the large pores in the totally deteriorated cement paste in the concrete composite. As a physical background of this treatment, the authors assume that the pore structure of the deteriorated cement paste would have similar characteristics to the soils as,

$$\delta = 0.395 \tanh \left\{ 4 \left(\log \left(r_{cp}^{peak} \right) + 6.2 \right) \right\} + 0.405 \quad (14)$$

$$\delta = 0 \text{ for } r_{cp}^{peak} \leq \frac{a_{Ca}}{2}.$$

where, r_{cp}^{peak} is the peak capillary pore radius [m] and a_{Ca} is an ion diameter parameter for calcium ions = 0.6×10^{-9} m. The peak pore radius in the Raleigh-Ritz distribution, does not as a parameter provide a direct expression of the fine pores in which interactions between ions and pore walls are prominent, but it does determine the shape of the pore size distribution. As a first approximation, constrictivity is modeled in this simplified manner. A detailed study of statistical processing for the connectivity of pores is required in the future. The effect of ion concentration will also need to be taken into account (Sato *et al.* 1995).

2.5 Variable pore structure caused by calcium leaching

It has been reported that the leaching of calcium leads to a coarse pore structure in the cement paste. This may accelerate calcium leaching. In this study, an increment

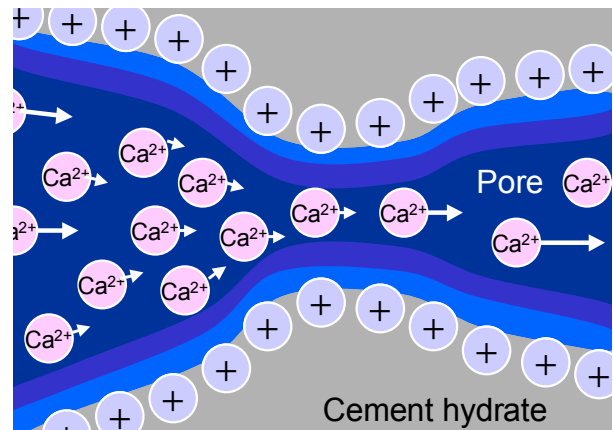


Fig. 7 Effect of electrostatic repulsion.

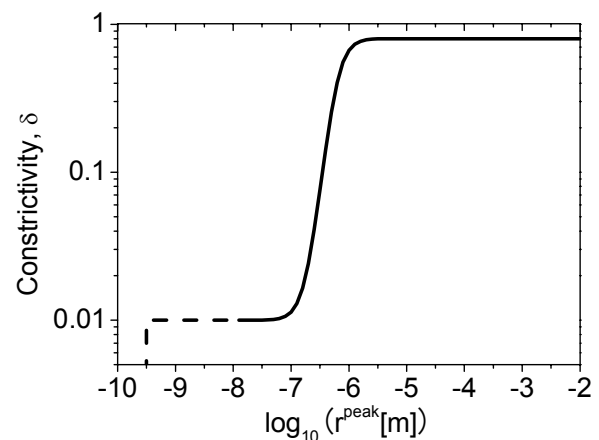


Fig. 8 Modeling of constrictivity.

in pore size and volume caused by the dissolution of calcium hydroxide and C-S-H gel is taken into account. That is, the change in pore structure and moisture re-distribution caused by calcium leaching is calculated by substituting the increased pore size and volume into the existing thermodynamic coupled analysis system.

The increased pore volume resulting from dissolution of calcium hydroxide is expressed as a volumetric decrease in calcium hydroxide, ΔV_{CH} , according to the following:

$$\Delta V_{CH} = \Delta m_{CH} / \rho_{CH}, \quad \Delta m_{CH} = \Delta C_{CH} M_{CH} \quad (15)$$

where, ΔV_{CH} is the volumetric decrease in calcium hydroxide due to leaching [m^3/m^3], Δm_{CH} is the decrease in mass of calcium hydroxide due to leaching [kg/m^3], ρ_{CH} is the density of calcium hydroxide ($=2.24 \times 10^3 [\text{kg}/\text{m}^3]$), ΔC_{CH} is the decrease in solid-phase calcium in the calcium hydroxide [mmol/m^3], and M_{CH} is the molecular mass of calcium hydroxide ($=74.1 \times 10^{-6} [\text{kg}/\text{mmol}]$).

The process of C-S-H gel dissolution is more complex than that of calcium hydroxide. In this study, the solid volume aside from that of the calcium hydrates and silicon dioxide is taken into account in the dissolution process. Then, the increase in pore volume due to dissolution of C-S-H gel is simply expressed by assuming a

linear relation with the amount of leached calcium as,

$$\Delta V_{CSH} = \frac{C_{CSH} - C_{solid}}{C_{CSH}} \cdot V_{CSH} \quad (16)$$

where, ΔV_{CSH} is the volumetric change in C-S-H gel [m^3/m^3], which means the increase in porosity caused by dissolution of C-S-H gel. V_{CSH} is the volume of C-S-H gel when dissolution is assumed to be zero. The volume V_{CSH} is obtained from the following expression:

$$V_{CSH} = V_{unhyd} + V_{hyd} - V_{SiO_2} \quad (17)$$

where, V_{unhyd} is the volume of und powder [m^3/m^3], V_{hyd} is the volume of hydrates [m^3/m^3], and V_{SiO_2} is the volume of silicon dioxide assumed not to be dissolved [m^3/m^3]. Thus, we have,

$$V_{unhyd} = (1 - \alpha) \frac{m_p}{\rho_p} \quad (18a)$$

$$V_{hyd} = \alpha m_p \left(\frac{1}{\rho_p} + \frac{\beta_p}{\rho_u} \right) \quad (18b)$$

$$V_{SiO_2} = \frac{Si \cdot M_{SiO_2}}{\rho_{SiO_2}} \quad (18c)$$

where, α is the average hydration degree, m_p is the mass of powder, ρ_p is the density of the powder, ρ_u is the density of the bound water in the hydrates ($=1.25 \times 10^3$ [kg/m^3]), β_p is the mass of the bound water per mass of hydrated powder [kg/kg], Si is the molecular amount of silicon [mmol/m^3], M_{SiO_2} is the molecular mass of silicon dioxide ($=60.1 \times 10^{-6}$ [kg/mmol]), and ρ_{SiO_2} is the density of silicon dioxide ($=2.20 \times 10^3$ [kg/m^3]). The amount of silicon in the cement is calculated from its mineral composition. The amount of silicon in fly ash and blast furnace slag is assumed to be 33.6% (JSCE 1998a) and 56.0% (JSCE 1998b), respectively. Unhydrated powder is not actually leached directly, since the leaching rate is much smaller than the hydration rate.

2.6 Differential time step

In order to numerically solve Equation (1), we need to calculate incremental changes in porosity, degree of saturation, and number of calcium ions in the liquid and solid phases in an infinitesimal time. In the analytical scheme, all are calculated as time-dependent variables associated with ambient conditions, cement hydration, and degradation due to leaching. These variables are interpolated between finite time steps to obtain a solution.

The increment in calcium ions in the liquid phase is discretized with respect to time as,

$$\frac{\partial}{\partial t} (\phi \cdot S \cdot C_{ion}) = \frac{\phi^{n+1} \cdot S^{n+1} \cdot C_{ion}^{n+1} - \phi^n \cdot S^n \cdot C_{ion}^n}{t^{n+1} - t^n} \quad (19)$$

where, t^{n+1} and t^n are the times [sec] at the $n+1^{\text{th}}$ step and n^{th} step, respectively. In this notation, the superscript denotes the time step. So, for example, ϕ^{n+1} represents the porosity at the $n+1^{\text{th}}$ step. The porosity in Equation (19) is obtained from the microstructure model over time. The degree of saturation is also obtained from the moisture model.

Next, the increment in calcium ions in the solid phase is expressed in the form of a finite difference as,

$$\begin{aligned} \frac{\partial C_{Solid}}{\partial t} &= \frac{C_{Solid}^{n+1} - C_{Solid}^n}{t^{n+1} - t^n} \\ &= \frac{f^{n+1}(C_{ion}^{n+1}) - f^n(C_{ion}^n)}{t^{n+1} - t^n} \end{aligned} \quad (20)$$

When calculating the solid calcium associated with the varying amount of calcium ions, a simplified piecewise linearity of solid-liquid equilibrium is not adopted. Rather, the full nonlinear relation is directly solved so as to maintain the accuracy of the numerical solution. That is because the strong coupling makes the isothermal solid-liquid equilibrium dynamically change with varying hydration, temperature, and chloride concentration over time (Fig. 9).

3. Verification

3.1 Immersion test

The proposed model was verified by comparing with immersion experiments. Block-shaped specimens were submerged in deionized water to accelerate calcium leaching. This method is able to quickly deliver more realistic results than immersion tests using cement powder.

In one experiment, the proposed model was used to simulate research by Watanabe *et al.* (2000). In their experiment, a cubic mortar specimen of $W/C=70\%$ was prepared. All three dimensions were 40mm. It was cured in the sealed condition for 42 days and then soaked in the deionized water. The water-to-solid volume ratio was 50.0. The water was replaced with new deionized water

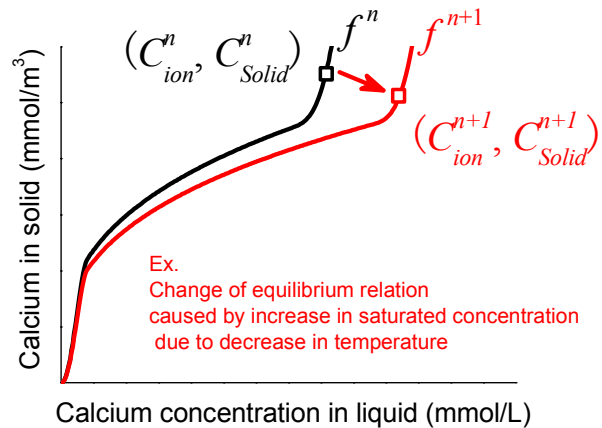


Fig. 9 Example of change in equilibrium relationship.

every three months. After 12 months of immersion, the distribution of remaining calcium in the specimen was measured using energy dispersion X-ray spectrometry (EDS). In the analysis, the concentration of calcium ions in the water was assumed to be 2 mmol/l to take into account the calcium remaining in the water. This value was determined based on the total amount of leached calcium ions. Here, hydroxide ions at a concentration of 4 mmol/l in the water are implicitly assumed to be balanced anion of cation (2 mmol/l calcium ions).

The experimental and simulated profiles of calcium distribution are shown in **Fig. 10**. The simulation indicates slightly greater deterioration than observed in the experiment. Given that a higher calcium concentration in the water is inevitable near the specimen, this small discrepancy is thought to be acceptable. For a stricter estimate, it would be necessary to integrate a simulation of hydro-dynamics for the surrounding water into the model.

The proposed model was also tested against a sodium chloride experiment carried out by Imoto *et al.* (2004). Cubic paste specimens of $W/C=40\%$ were prepared. All three dimensions were 40 mm. After casting, the specimens were cured at high humidity for one day followed by wetting for 27 days. The water-to-solid volume ratio was 50.0. Three kinds of water were used for immersion tests: deionized water, 0.28 mol/l sodium chloride solution, and 0.56 mol/l sodium chloride solution. The water was replaced every three months. After four years of immersion, the amount of residual calcium hydroxide and the total porosity were measured.

Figure 11 shows the experimental and simulated results for calcium hydroxide while **Fig. 12** gives the porosity results. Compared with deionized water soaking, immersion in sodium chloride led to accelerated loss of calcium hydroxide and rise in porosity. Further, the concentration of sodium chloride did not affect the results significantly in these cases. The model simulates these tendencies as a result of taking into account the effect of chloride ions on the solubility product.

3.2 Sensitivity analysis of influence of temperature on calcium leaching

The influence of temperature is considered in formulating the solubility product of calcium hydroxide and the diffusivity of calcium ions. Sensitivity to temperature is reviewed for the case of G50, which has a W/C ratio of 50%. The mix proportion is shown in **Table 1**.

First, the temperature sensitivity of the equilibrium relation is considered. In the simulation, after curing at 20°C for 80 days, the temperature was changed to 10, 20, 40, 60°C in order of time under the sealed condition. The applied temperature history is shown in **Fig. 13a**. As a sealed boundary is assumed, the total amount of calcium is constant. **Figure 14** shows sensitivity analysis with respect to the temperature-dependent solubility product of calcium hydroxide. **Figure 13b** shows the change in calcium ion concentration and **Fig. 13c** is the response of

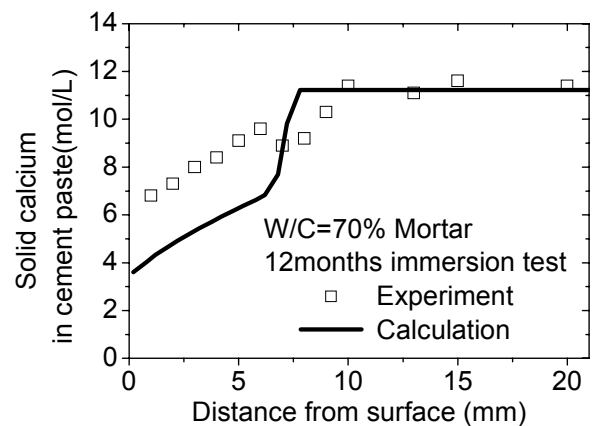


Fig. 10 Change in solid calcium due to leaching (immersion test).

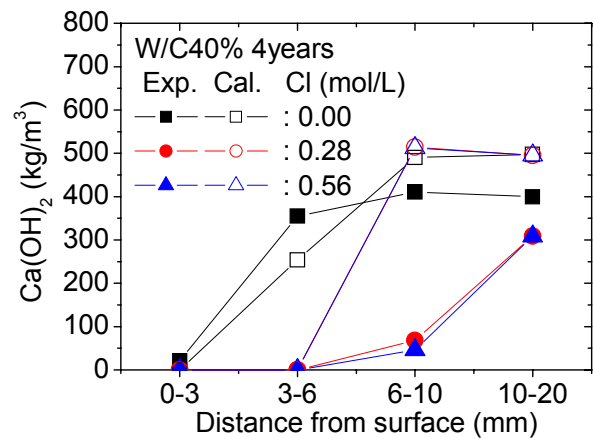


Fig. 11 Change in calcium hydroxide (immersion test).

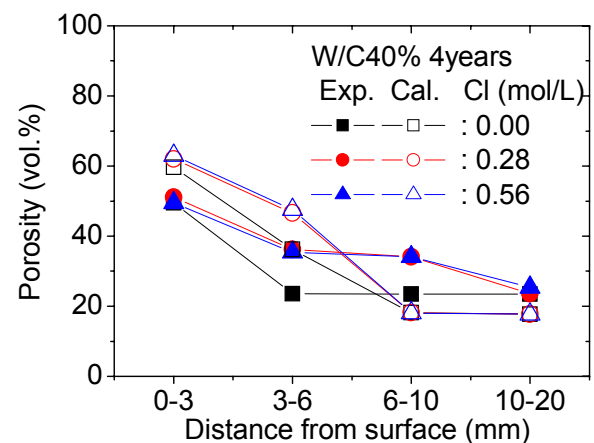


Fig. 12 Change in porosity (immersion test).

total and solid calcium. When the temperature increases, the calcium ion concentration decreases with the fall in solubility product, resulting in increased solid calcium. The total amount of calcium remains unchanged with changing temperature.

Second, the influence of temperature on long-term calcium leaching is reviewed numerically. In this analysis, concrete specimens were exposed to water with a

calcium ion concentration of 2 mmol/l at different tem-

Table 1 Mix proportion of concrete for analysis.

No	W/P	Unit mass (kg/m ³)				
		W	C	FA	S	G
G25	25	190	760	0	600	775
G50	50	190	380	0	700	988
F50	50	190	304	76	700	950

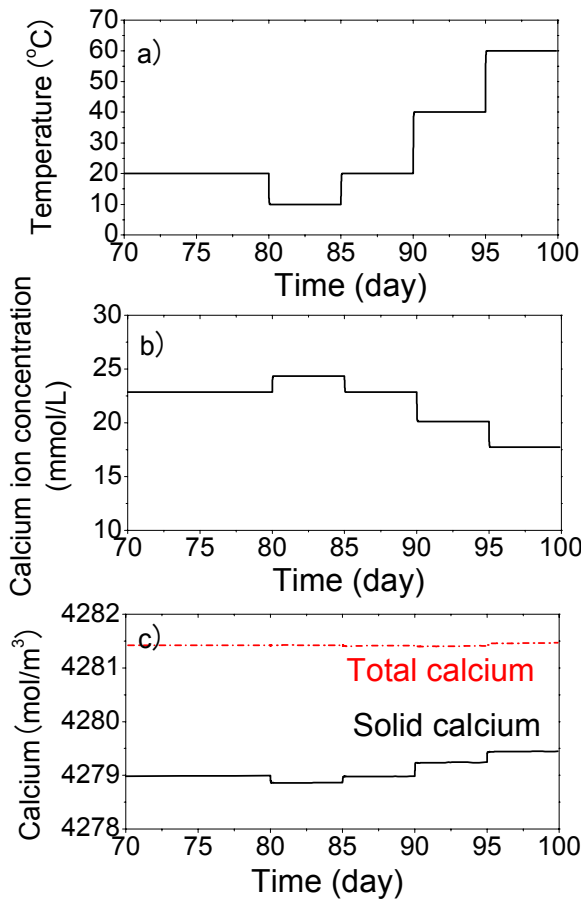


Fig. 13 Influence of temperature on phase change of calcium.

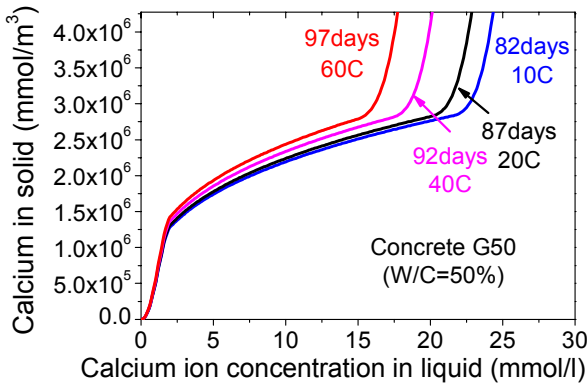


Fig. 14 Influence of temperature on equilibrium relationship.

peratures after sealed curing at 20°C for 28 days. The analysis target was again G50 in **Table 1**. **Figure 15** shows the results after 10,000 years of accelerated aging. The results indicate that an increase in temperature accelerates leaching. This increase causes a declining solubility product (**Fig. 14**) and rising diffusivity (**Table 2**), respectively. These changes have different effects on calcium leaching. Whereas the decrease in solubility product reduced calcium leaching, the increase in diffusivity accelerates the leaching. In the proposed equilibrium model, the effect of the reduced solubility product on equilibrium becomes less in the leaching process of C-S-H than in the process of calcium hydroxide (**Fig. 14**). Since C-S-H leaching process plays a major role in the long-term deterioration of the solid, the effect of the higher diffusivity is thought to be significant in this analysis.

3.3 Sensitivity analysis of influence of water-to-cement ratio on calcium leaching

In order to investigate the influence that *W/C* has on long-term degradation caused by calcium leaching, sensitivity analysis was performed using the proposed model as well as with a trial model. The targets of the analysis were G25 (*W/C*=25%) and G50 (*W/C*=50%). Both contained the same unit mass of water: 190 kg/m³. The mix proportions are shown in **Table 1**. In the analysis, the concrete specimens were exposed to water with 2 mmol/l of calcium ions after sealed curing for 28 days. The temperature was fixed at 20°C. In order to discuss interrelationships between increased porosity caused by calcium leaching and progress with hydration, additional calculations were performed using a trial model. In this sensitivity analysis of the trial model, the increase in porosity related to leaching is intentionally neglected in

Table 2 Influence of temperature on diffusivity.

Temperature	10°C	20°C	40°C
$\frac{\delta}{\tau} D_{ion}$ (m ² /s)	6.13E-12	7.79E-12	1.28E-11

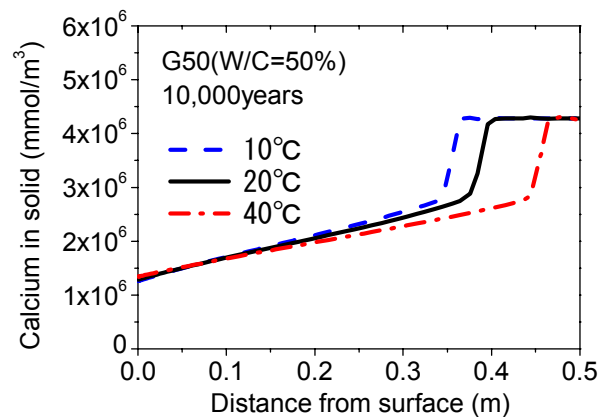


Fig. 15 Influence of temperature on long-term calcium leaching.

the hydration model. The porosity affects the amount of free water, which in turn influences the hydration rate. That is the trial model does not take into account additional hydration associated with the change in pore structure caused by calcium leaching.

Figure 16 shows the analytical results after 10,000 years. Both the proposed model and the trial model show that a low W/C results in smaller deterioration depth. In the case of G50 ($W/C=50\%$), both models give almost the same results. In the case of G25 ($W/C=25\%$), however, the proposed model in which increasing porosity with leaching is taken into account exhibits less degradation compared with the trial model.

When the W/C is below 40%, such as with specimen G25, the initial mixing water is not enough to allow full

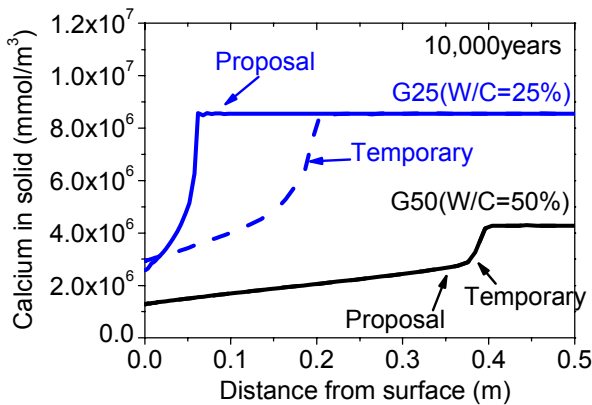


Fig. 16 Influence of W/C on long-term calcium leaching.

hydration of the cement. As free water is short during the hydration of such low W/C concrete, unhydrated cement remains. Then, as leaching proceeds, the newly created pore spaces that result may act as free space for additional hydration. Consequently, unhydrated cement starts to react with existing water (Fig. 17). This additional hydration causes the pore structure to become dense once again in a kind of self-curing system for low W/C concrete. In the case of normal or higher W/C , this self-curing is not observed since there is no unhydrated cement. The changes in degree of hydration illustrated in Figs. 18 and 19 clearly show the mechanism of self-curing as calcium leaching takes place. The proposed model calculates significant additional hydration of low W/C concrete as calcium leaching occurs. This self-curing system in low W/C concrete can be predicted only by a model that considers the strong coupling between hydration and changes to the pore structure. Whatever a further verification for the self-curing phenomenon is, the authors recognize that the analytical system and its predictions show the higher possibility of efficiently using low W/C concrete as a high-performance material for nuclear waste management.

3.4 Sensitivity analysis of influence of fly ash on calcium leaching

It has been reported that fly ash (FA) reduces degradation related to calcium leaching (Yokozeki 2004). In this section, the effect of FA on calcium leaching is investigated using the proposed model. The specimens subjected to analysis (G50 and F50) have a common mix

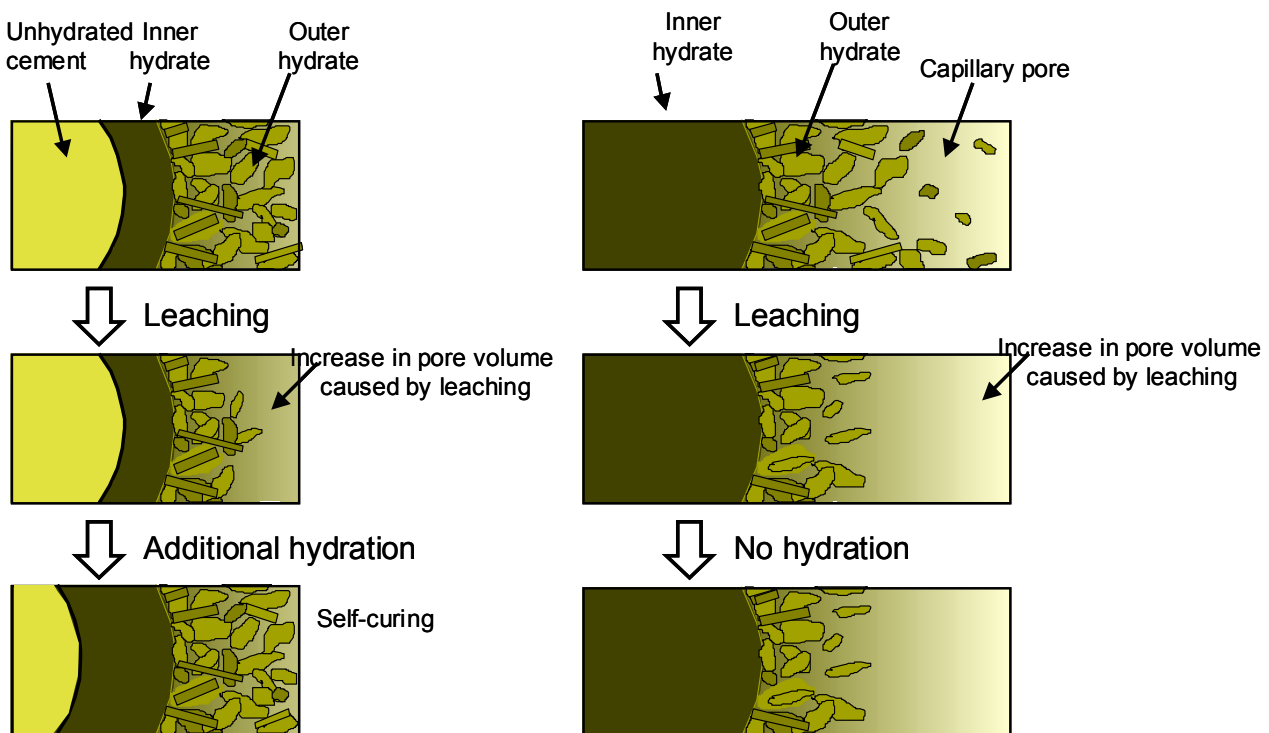


Fig. 17 Relation between hydration and calcium leaching.

proportion with $W/P=50\%$ and a unit mass of water of 190 kg/m^3 . Two replacement ratios of FA (0% and 20%) were studied. The mix proportions are shown in **Table 1**.

The calculated distributions of solid calcium in the concrete after 10,000 years are shown in **Fig. 20**. As this

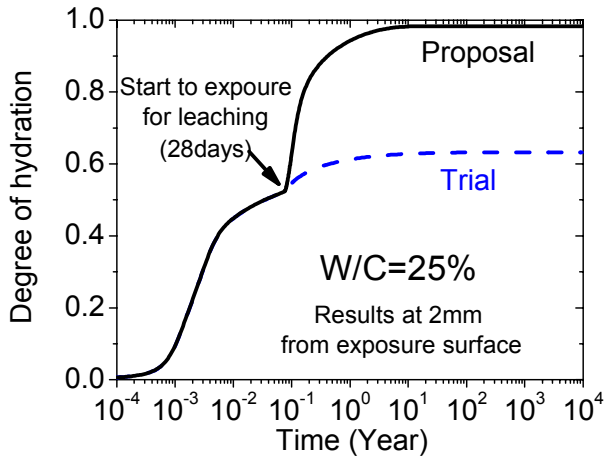


Fig. 18 Change in hydration degree due to leaching ($W/C=25\%$).

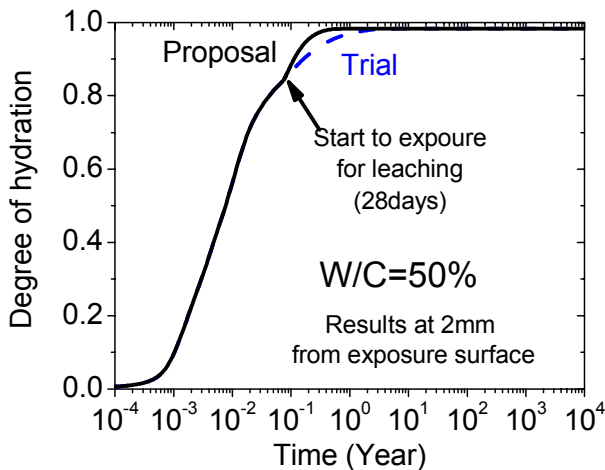


Fig. 19 Change of hydration degree due to leaching ($W/C=50\%$).

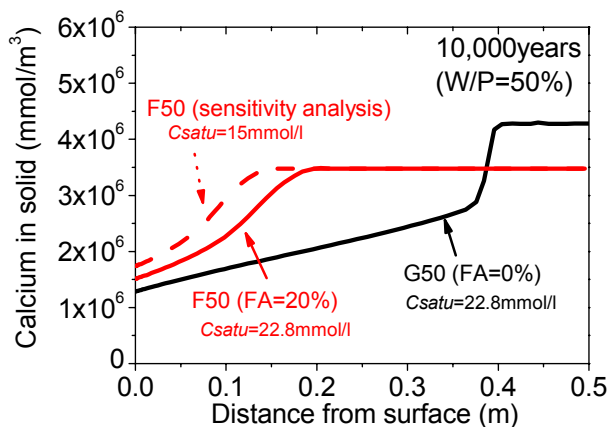


Fig. 20 Influence of fly ash on long-term calcium leaching.

figure makes clear, concrete with 20% FA has greater resistance to calcium leaching. This is for two reasons: it has a different calcium solid-liquid equilibrium and a different ultimate micro-pore structure. The use of FA leads to a different equilibrium relationship (**Fig. 21**), since the pozzolanic reaction consumes calcium hydroxide, which has high solubility in pore water. The ratios of calcium hydroxide to total solid calcium were 32.4% in G50 (FA 0%) and 13.4% in F50 (FA 20%) in the sound part of the concrete after 10,000 years, respectively. In addition to the change in the equilibrium relationship, the micro-pore structure becomes denser with the use of FA. This trend can be seen in **Fig. 22**. In the case of F50 with FA, the capillary pores disappear, resulting in lower diffusivity, as shown in **Table 3**. They show that 20% use of FA reduced the effective diffusion coefficient to almost half in this analysis. These values of the coefficients almost agree with the experimental results measured by electrical potential methods (Horiuchi *et al.* 1998).

On the other hand, the coefficient of FA concrete is much smaller compared to the experimental results measured by diffusion cell tests (Uchikawa 1985). The effective diffusion coefficient of the concrete with 20%

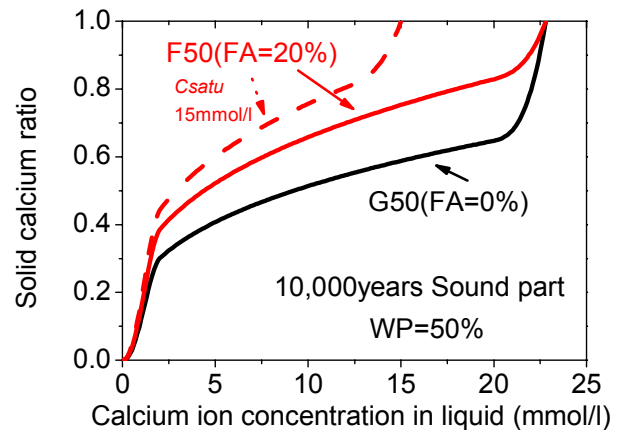


Fig. 21 Influence of fly ash on equilibrium relation.

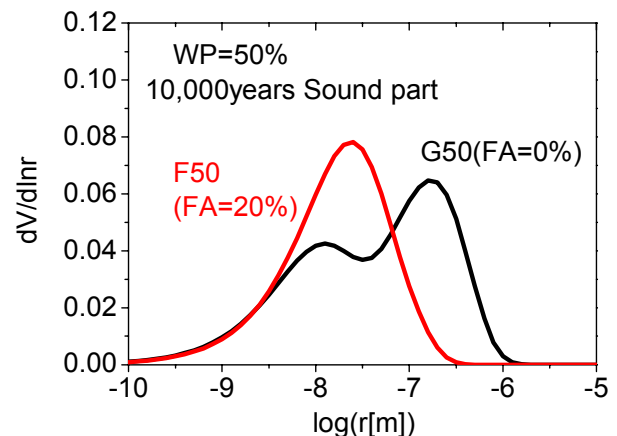


Fig. 22 Influence of fly ash on porosity distribution.

Table 3 Influence of fly ash on diffusivity.

No	G50	F50
$\frac{\delta}{\tau} D_{ion}$ (m ² /s)	7.79E-12	3.55E-12

Table 4 Deterioration depth after 82 weeks.

No	Experiment (mm)	Calculation (mm)
OPC	2.4	1.8
OPC with 30% fly ash	0.6	1.6

FA is about one tenth of the coefficient of concrete without FA. The reason of the large decrease in the coefficients by the diffusion cell tests is thought to be the increase in the electrical interactions between ions and pore wall, because the electrical potential method may mask the internal electrical interaction due to the large external electric charge.

In order to investigate the adequacy of the effective diffusion coefficient in the proposed model, a comparison of deterioration depth between the experimental results by Yamamoto and Hironaga (2006) and analytical results by the proposed model was made. In the experiments, the specimens of cement paste were immersed in the deionized water for 82 weeks after the curing under 50 °C for 91 days in order to investigate the effect of FA on the calcium leaching. The water-to-binder ratio was 40% and the replacement ration of FA was 30%. **Table 4** shows the deterioration depth from the exposure surface in the analytical and experimental results. In the case of FA, the calculated deterioration depth is much larger than the measured depth in the experiment. This indicates that the decrease in the effective diffusion coefficients calculated for FA concrete is underestimated. The detailed investigation of the effective diffusion coefficient is needed in future.

Finally, the effect of a decrease in calcium ion solubility in the equilibrium relation is investigated by using G50 and F50, since it is reported that the solubility decreases in the presence of FA (Yokozeki 2004). Although the calculated effective diffusion coefficient for FA concrete in this analysis is larger than the reality, the more qualitative investigation on the phase-equilibrium relation is thought to be possible. In this sensitivity analysis at 20°C, the saturated concentration of calcium ions in F50 was tentatively changed to 15.0 mmol/l based on past research, whereas the calculated value in the proposed model was 22.8 mmol/l (**Fig. 20**). The result for residual calcium in the solid phase is shown in **Fig. 21**. By decreasing the saturated concentration in the solid-liquid equilibrium, deterioration was reduced. The effect of decreasing the saturated concentration was, however, not as significant compared as the effect of changing the amount of calcium hydroxide and porosity, which are automatically taken into account in the proposed system.

4. Conclusions

The leaching of calcium from cement hydrates in concrete was simulated using a model of the micro-pore structure in order to study degradation related to ion pathways. In the proposed methodology, a model for calcium leaching was installed into an existing thermodynamic analytical system so as to take into account the effects of hydration, micro-pore structure, moisture profile, and chloride concentration on leaching. The elements of the research are outlined below.

(a) The influence of temperature on calcium leaching was numerically investigated. An increase in temperature was found to accelerate degradation through an accompanying increase in diffusivity. The lower solubility product that results from the increase in temperature was not found to be significant in this analysis.

(b) The influence of chloride ions was investigated. In the proposed model, the acceleration of leaching in the presence of sodium chloride is expressed in terms of an increase in the solubility product.

(c) The influence of water-to-cement, *W/C*, was numerically investigated. The proposed model revealed that low *W/C* concrete has a high resistance to leaching. The model further showed that unhydrated cement in low *W/C* concrete reacts with free water in additional space that results from calcium leaching. This additional hydration corrected the damage caused to the micro-pore structure.

(d) The influence of fly ash on calcium leaching was investigated. Although the analytical prediction slightly underestimated the experimental results, the proposed model is able to simulate the reduced leaching degradation of fly ash concrete resulting from the decrease in calcium hydroxide and the dense micro-pore structure associated with the pozzolanic reaction.

Acknowledgments

The authors acknowledge the valuable advice provided by Dr. Bruno Gérard of OXAND S.A. Appreciation is also extended to Mr. S. Nakane for his assistance in this work. This research was financially supported by Grant-in-Aid for Scientific Research (Young Scientists B) No.16760358 and (S) No.15106008.

References

- Atkinson, A. and Nickerson, A. K. (1984). "The diffusion of ions through water-saturated cement." *Journal of Materials Science*, 19, 3068-3078.
- Berner, U. R. (1988). "Modelling the incongruent dissolution of hydrated cement minerals." *Radiochimica Acta*, 44/45, 387-393.
- Buil, M., Revertegat, E. and Oliver, J. (1992). "A model of the attack of pure water or under saturated lime solutions on cement." ASTM STP 1123, 227-241.
- CSJ, (2004). "Science Handbook." Chemical Society of Japan, Maruzen. (in Japanese)
- Maekawa, K., Chaube, R. P. and Kishi, T. (1999).

- “Modelling of concrete performance.” London: E&FN SPON.
- Gérard, B., Le Bellego, C. and Bernard, O. (2002). “Simplified modeling of calcium leaching of concrete in various environments.” *Materials and Structures*, 35, 632-640.
- Horiuchi, Z., Sugiyama, T., Tsuji, Y. and Hashimoto, C. (1998). “A study on the pore structure of concretes containing fly ash by electrical potential method.” *Proceedings of Japan Concrete Institute*, 20(1), 203-208. (in Japanese)
- Imoto, H., Kurashige, R., Hironaga, M. and Yokozeki, K. (2004). “Leaching behavior of Portland cement hydrate in sodium chloride solution.” *Proceedings of Japan Concrete Institute*, 26(1), 903-908. (in Japanese)
- Ishida, T. and Maekawa, K. (2000). “An integrated computational system for mass/energy generation, transport, and mechanics of materials and structures.” Japan Society of Civil Engineers, *Concrete library of JSCE*, 36, 129-144.
- JSCE, (1998a). “Long-term research on carbonation and corrosion of concrete using fly ash (Final report).” Tokyo: Japan Society of Civil Engineers, *Concrete library*, 64, 16. (in Japanese)
- JSCE, (1998b). “Recommendation for design and construction of concrete using blast furnace slag.” Tokyo: Japan Society of Civil Engineers, *Concrete library*, 63, 56-57. (in Japanese)
- Maekawa, K., Ishida, T. and Kishi, T. (2003). “Multi-scale modeling of concrete performance – Integrated material and structural mechanics.” *Journal of Advanced Concrete Technology*, 1(2), 91-126.
- Petersen, E. E. (1958). “Diffusion in a pore of varying cross section.” *A. I. Ch. E. Journal*, 4(3), 343-345.
- Sato, H., Yui, M. and Yoshikawa, H. (1995). “Diffusion behavior for Se and Zr in sodium-bentonite.” *Proceedings of Materials Research Society Symposium*, Vol.353, 269-276.
- Uchikawa, H. (1985). “Effect of blast furnace slag and fly ash on the diffusivity of alkali ions in hardened cement paste.” *Cement and Concrete*, No.460, 20-27. (in Japanese)
- Van Brakel, J. and Heertjes, P. M. (1974). “Analysis of diffusion in macroporous media in terms of a porosity, a tortuosity and a constrictivity factor.” *International Journal of Heat and Mass Transfer*, 17, 1093-1103.
- Watanabe, K., Yokozeki, K., Otsuki, N. and Daimon, M. (2000). “Experimental investigation for analysis of calcium leaching of cementitious materials.” *Proceedings of Japan Concrete Institute*, 22(1), 217-222. (in Japanese)
- Yamamoto, T. and Hironaga, M. (2006). “Evaluation of leaching process of cementitious materials for engineered barrier system.” *Proceedings of Japan Concrete Institute*, 28(1), 713-718. (in Japanese)
- Yokozeki, K., Watanabe, K., Hayashi, D., Sakata, N. and Otsuki, N. (2003). “Modeling of ion diffusion coefficients in concrete considering hydration and temperature effects.” *Concrete Library International*, 42, 105-119.
- Yokozeki, K. (2004). “Long-term durability design of 1,000-year level on leaching of cement hydrates from concrete.” Thesis (Ph.D), Tokyo Institute of Technology. (in Japanese)